1

Associations between ADHD symptom remission and white

matter microstructure: a longitudinal analysis

4

A.E.M.Leenders[1*], C.G.Damatac[1,2*], S.Soheili-Nezhad[1,2], R.J.M.Chauvin[1,2],

M.J.J.Mennes[1,2], M.P.Zwiers[1,2], D.vanRooij[1,2], S.E.A.Akkermans[1,3], J.Naaijen[1,2],

B.Franke[3,4], J.K.Buitelaar[1,2,5], C.F.Beckmann[1,2,6], E.Sprooten[1,2]

[1]Centre for Cognitive Neuroimaging, Donders Institute for Brain, Cognition and Behaviour, Radboud University, Nijmegen, the Netherlands; [2]Department of Cognitive Neuroscience, Donders Institute for Brain, Cognition and Behaviour, Radboud University Medical Centre, Nijmegen, the Netherlands; [3]Department of Human Genetics, Donders Institute for Brain, Cognition and Behaviour, Radboud University Medical Centre, Nijmegen, the Netherlands; [4]Department of Psychiatry, Donders Institute for Brain, Cognition and Behaviour, Radboud University, Nijmegen, the Netherlands; [5]Karakter Child and Adolescent Psychiatry University Centre, Nijmegen, the Netherlands; [6]Centre for Functional MRI of the Brain, University of Oxford, Oxford, UK

* Authors contributed equally to this work.

21 ## Abstract

22   **Background:** Attention-deficit hyperactivity disorder (ADHD) is associated with white matter

23   (WM) microstructure. Our objective was to investigate how WM microstructure is

24   longitudinally related to symptom remission in adolescents and young adults with ADHD.

25   **Methods:** We obtained diffusion-weighted imaging (DWI) data from 99 participants at two

26   time points (mean age baseline: 16.91 years, mean age follow-up: 20.57 years). We used voxel-

27   wise Tract-Based Spatial Statistics (TBSS) with permutation-based inference to investigate

28   associations of inattention (IA) and hyperactivity-impulsivity (HI) symptom change with

29   fractional anisotropy (FA) at baseline, follow-up, and change between time points. **Results:**

30   Remission of combined HI and IA symptoms was significantly associated with reduced FA at

31   follow-up in the left superior longitudinal fasciculus and the left corticospinal tract (CST)

32   (P_{FWE}=0.038 and P_{FWE}=0.044, respectively), mainly driven by an association between HI

33   remission and follow-up CST FA (P_{FWE}=0.049). There was no significant association of

34   combined symptom decrease with FA at baseline or with changes in FA between the two

35   assessments. **Conclusions:** In this longitudinal DWI study of ADHD using dimensional

36   symptom scores, we show that greater symptom decrease is associated with lower follow-up

37   FA in specific WM tracts. Altered FA thus may appear to follow, rather than precede, changes

38   in symptom remission. Our findings indicate divergent WM developmental trajectories

39   between individuals with persistent and remittent ADHD, and support the role of prefrontal

40   and sensorimotor tracts in the remission of ADHD. **Keywords:** ADHD; white matter; dMRI;

41   remission; longitudinal. **Abbreviations:** white matter(WM), NeuroIMAGE1(TP1),

42   NeuroIMAGE2(TP2)

Introduction

Attention-deficit/hyperactivity disorder (ADHD) is a common neuropsychiatric disorder characterized by developmentally inappropriate levels of inattention (IA) and/or hyperactivity-impulsivity (HI), with an estimated prevalence of 5% in children and adolescents and 2.5% in adults(Faraone et al., 2015). For many, ADHD begins in childhood, but the long-term clinical course of ADHD varies widely between individuals(American Psychiatric Association, 2013). Prospective studies suggest that although only 15% of children with ADHD continue to fully meet diagnostic criteria in adulthood, 60-70% of them retain impairing symptoms in adulthood(Faraone et al., 2015). ADHD diagnosis has been associated with altered patterns of brain structure and function, however the neural mechanisms related to symptom progression (i.e. remission vs. persistence) have not yet been fully unraveled (Aoki, Cortese, & Castellanos, 2018; Damatac et al., 2020; Francx, Zwiers, et al., 2015; Franke et al., 2018; Hoogman et al., 2017). Understanding this could help develop and tailor treatments to benefit long-term outcomes for children with ADHD.

The underlying neural mechanisms that drive symptom remission may be distinct from those that drive ADHD onset, thus the brains of remitted individuals could be methodologically differentiated from those of people who were never diagnosed with ADHD(Halperin & Schulz, 2006). Here, we refer to symptom remission as a dimensional concept, as a decrease in symptom severity between two time-points. Symptom remission can be driven by a number of neurodevelopmental mechanisms which are not mutually exclusive. Previous hypotheses suggest that disorder onset is characterized by a fixed anomaly or 'scar', while symptom remission or persistence is associated with brain maturation and normalization, or compensation and reorganization(Sudre, Mangalmurti, & Shaw, 2018). The trajectories of remission and persistence from childhood through adulthood occur in parallel to or in interaction with other neurodevelopmental processes (e.g.development of executive functions).

68   The development of frontal and temporal areas engaged in emotional and cognitive

69   processes does not plateau until adulthood, which coincides with the typical age range of

70   ADHD symptom remission(Faraone et al., 2015; Lebel & Deoni, 2018). Maturation in these

71   regions may compensate for the initial childhood development of ADHD symptoms through

72   top-down regulatory processes, leading to eventual symptom remission(Halperin & Schulz,

73   2006). Therefore, longitudinal cohort studies are essential to dissect the upstream, parallel, or

74   downstream brain mechanisms in reference to symptom remission. Compared to a cross-

75   sectional approach, a longitudinal design provides not only unique insights into the temporal

76   dynamics of underlying biological processes, but also increased statistical power by reducing

77   between-subject variability(Madhyastha et al., 2014).

78   Neurodevelopmental mechanisms underlying the variable long-term course of ADHD

79   may be partly traceable using neuroimaging. Healthy brain development has been characterized

80   using structural and functional magnetic resonance imaging (MRI), showing trajectories across

81   the lifespan of regional volumes and activity/connectivity, respectively(Brouwer et al., 2020;

82   van Duijvenvoorde, Westhoff, de Vos, Wierenga, & Crone, 2019). Those that have applied

83   diffusion, magnetization transfer, relaxometry, and myelin water imaging methods have also

84   demonstrated consistent, rapid white matter (WM) microstructural changes in the first three

85   years of life, reflecting increased myelination or axonal packing(Lebel & Deoni, 2018). These

86   changes continue throughout adolescence and are associated with corresponding age-related

87   changes in gray matter(Giorgio et al., 2008). However, regarding later childhood and

88   adolescence, the paucity of congruous findings in other WM imaging modalities besides

89   diffusion weighted imaging (DWI) suggests that changes are primarily related to myelination

90   and axonal packing(Lebel & Deoni, 2018). With age, WM increases in overall volume,

91   becoming more myelinated in a region-specific fashion and reaching peak values later in

92   life(Kochunov et al., 2012; Paus et al., 2001). The rate of development differs between WM

93 regions, progressing in an outward, central-to-peripheral direction, wherein sensory and motor

94 regions generally mature the earliest.

95   DWI studies have revealed WM microstructural abnormalities in ADHD, specifically

96 using fractional anisotropy (FA), which is the metric we focus on here(Aoki et al., 2018;

97 Damatac et al., 2020; van Ewijk et al., 2014; Francx, Oldehinkel, et al., 2015; Shaw et al.,

98 2015; Sudre et al., 2018). DWI reveals information about anatomical connectivity in the brain

99 *in vivo* by measuring the directionality of water diffusion in WM tracts, thus enabling

100 inferences about underlying brain mechanisms by quantifying associated changes in

101 (inter)cellular space(Beaulieu, 2002; van Ewijk et al., 2014). FA is an indirect measure of

102 microstructural integrity—sensitive to myelination, parallel organization and fiber bundle

103 density. A systematic meta-analysis of case-control DWI studies in ADHD found that lower

104 FA in ADHD has mostly been reported in interhemispheric, frontal and temporal regions—

105 however, higher FA has also been found in similar areas(Aoki et al., 2018). Given these

106 previous WM associations with ADHD and the brain's maturation in those same areas during

107 an age range typical for symptom remission, the next step is to determine how WM

108 microstructural alterations coincide with remission versus persistence of ADHD symptoms

109 over time.

110   Not many longitudinal studies have examined the neurobiological underpinnings of

111 symptom remission in WM—and none have longitudinally applied DWI. While there are no

112 previous studies with longitudinal DWI measurements, there have been some clinical

113 longitudinal studies with one DWI measurement. A follow-up DWI analysis three decades after

114 diagnosis supports the theory of the disorder as an enduring neurobiological trait independent

115 of remission; both remittent and persistent probands with an ADHD diagnosis in childhood

116 had widespread reduced FA compared to those who did not have childhood ADHD(Cortese et

117 al., 2013). Conversely, a network connectivity analysis of two clinical assessments and one

118   resting-state functional MRI measurement at follow-up pointed to the presence of

119   compensatory mechanisms that aid symptomatic remission in prefrontal regions and the

120   executive control network: higher connectivity at follow-up was associated with HI decreases

121   (Francx, Oldehinkel, et al., 2015). A study performed with a sample overlapping with the

122   current study (but at an earlier sampling time with mean age 11.9-17.8 years) found, somewhat

123   counterintuitively, that more HI symptom remission was associated with lower FA in the left

124   corticospinal tract (lCST) and left superior longitudinal fasciculus (lSLF) at follow-up(Francx,

125   Zwiers, et al., 2015). This previous study included clinical data from two time-points and only

126   one DWI time-point.

127   Our current investigation is a continuation of our earlier DWI work in this cohort, and

128   extends upon it in three ways. First, by capturing an older age range, we have a more complete

129   picture of symptom remission (mean age range: 16.91-20.57 years; Figure 1 illustrates how our

130   study chronologically relates to that of Francx *et al.*(2015). Second, DWI measurements at two

131   time-points allow for a more thorough investigation of the chronology and mechanisms of FA

132   development in relation to symptom remission. Third, we used Permutation Analysis of Linear

133   Models(PALM), a newly available permutation-based analysis technique, to account for the

134   family structure in our sample(Winkler, Webster, Vidaurre, Nichols, & Smith, 2015). We

135   aimed to examine whether symptom remission may be underpinned by WM alterations as

136   adolescents with ADHD develop into adulthood. Given our longitudinal DWI data, we were

137   able to distinguish between (1) pre-existing WM features that predict the likelihood of

138   symptoms to remit or persist, (2) WM changes over time that occur concurrently with symptom

139   change, and (3) WM alterations that may be a (direct or indirect) downstream consequence of

140   symptom remission versus persistence.

141   **Methods**

142   *Participants*

143   Clinical and MRI data were collected in two waves from probands with childhood ADHD,

144   their first-degree relatives, and healthy families: NeuroIMAGE1(TP1) and

145   NeuroIMAGE2(TP2)(Müller et al., 2011a, 2011b; von Rhein et al., 2015). The current study

146   included probands, affected and unaffected siblings, and healthy controls who participated in

147   both TP1 and TP2 and had DWI data from both waves(N=120). After we excluded

148   subjects(Figure S1), there were 99 participants from 65 families in our final sample (see

149   characteristics in Table 1). For both time-point groups, there were no differences between the

150   participants included in the current analysis and the complete sample on measures of ADHD

151   severity, age, and sex(P>0.05). We normalized head motion z-scores after excluding outliers.

152   Global FA at TP1, TP2, and the difference between TP1 and TP2 were normally distributed.

153   Given the longitudinal design of our study, we did not split our participants into cases

154   versus controls; there were those who were diagnosed as unaffected at both time-points, as well

155   as those who had a symptom score of zero in all dimensions at both time-points (Figure S2).

156   Our sample includes controls, or people who do not have (subthreshold) ADHD; however, this

157   group of people changed between the waves of the study (Figure S3). Some individuals

158   originally recruited as controls or unaffected siblings developed ADHD at a later time point

159   and others recruited as patients remitted. Moreover, ADHD may be operationalized as a

160   continuous trait rather than a binary diagnostic variable, especially in longitudinal studies

161   (Lahey & Willcutt, 2010; Marcus & Barry, 2011). In a previous cross-sectional study we

162   specifically showed that, compared to categorical diagnoses, continuous symptom measures

163   were more sensitive to diffusion-weighted brain features in this sample (Damatac et al., 2020).

164   Therefore, we focus on participants' ADHD symptom scores in all models, thus optimizing our

165   design and methods for capturing the dynamic and continuous nature of the ADHD spectrum

166   throughout adolescence.

Clinical measurements

168   Conners Parent Rating Scale(CPRS) questionnaires were used to assess the severity of 27

169   inattention(IA) and hyperactive-impulsive(HI) symptoms at TP1 and TP2(Conners et al.,

170   1999). We used CPRS instead of the self-rated report because it was the consistent measure

171   across waves and ages. We used raw CPRS scores to increase the distribution width, and

172   analyzed HI, IA, and combined symptom scores per subject, per time-point. Here, we define

173   symptom change as the score difference:$\Delta CPRS = CPRS_{TP1} - CPRS_{TP2}$. Thus, a more positive Δ

174   value indicates more symptom improvement.

Data acquisition and DWI pre-processing

176   MRI data were acquired with a 1.5-Tesla AVANTO scanner(Siemens, Erlangen, Germany).

177   The scanner was equipped with an 8-channel receive-only phased-array head coil. Whole-brain

178   diffusion-weighted images were collected(twice refocused pulsed-gradient spin-echo EPI; 60

179   diffusion-weighted directions spanning an entire sphere; b-value $1000s/mm^2$; 5 non-diffusion

180   weighted images; interleaved slice acquisition; TE/TR=97/8500ms; GRAPPA-acceleration

181   factor 2; no partial Fourier; voxel size 2x2x2.2mm). DWI acquisition parameters are described

182   in detail elsewhere(von Rhein et al., 2015).

Longitudinal TBSS

184   We performed whole brain voxel-wise analyses with Tract-Based Spatial Statistics

185   (TBSS)(Smith et al., 2006). Our study's longitudinal design necessitated an analysis pipeline

186   that considered how within-subject changes may be greater than between-subject changes;

187   intra-subject data alignment across time brings extra difficulty compared to cross-subject

188   nonlinear registration to common space. We used a bespoke pipeline adapted from others to

189   create non-biased individual subject templates(Madhyastha et al., 2014). Figure 2 summarizes

190   our pipeline(detailed in Figure S1).

191   *Statistical analysis*

192   We constructed three general linear models for our voxel-wise analyses (Table S1). We kept

193   difference in raw CPRS score(ΔCPRS) as a constant predictor, while separately testing FA at

194   baseline(FA_{TP1}), follow-up(FA_{TP2}), and the difference between TP1 and TP2 (ΔFA) as

195   dependent variables. Our covariates included sex, normalized head motion(framewise

196   displacement) at respective time point(s), age at TP1, age difference between TP1 and TP2,

197   and CPRS symptom score at TP1(Table S1, Figure S4). Our main analyses first examined

198   combined symptom scores and, if significant, subsequent analyses examined whether effects

199   were driven by HI or IA.

200   We used PALM to account for the lack of independence in the data due to sibling

201   relationships and shared variance between families, constraining permutation tests between

202   families of the same sizes(Winkler, Ridgway, Webster, Smith, & Nichols, 2014). We designed

203   multi-level exchangeability blocks which did not allow permutation among all individuals;

204   permutations were constrained both at the whole-block level (i.e. permute between families of

205   the same size) and the within-block level (i.e. permute within families)(Figure S5). We

206   corrected for multiple testing by running 5000 permutations and threshold-free cluster

207   enhancement(TFCE) as implemented in PALM, part of the FSL toolbox

208   (https://fsl.fmrib.ox.ac.uk/fsl/fslwiki/PALM)(Smith & Nichols, 2009). Results with TFCE-

209   corrected $P<0.05$ were considered statistically significant. All tests used the standard parameter

210   settings for height, extent, and connectivity: H=2, E=1, C=26. We used the Johns Hopkins

211   University DTI-based WM atlas (https://fsl.fmrib.ox.ac.uk/fsl/fslwiki/Atlases) to relate

212   significant clusters to known WM tracts.

Results

Symptom change over time

In Table 1, we present mean symptom scores for HI, IA, and combined (HI+IA). Combined symptom scores significantly decreased over time ($t(98)=4.884$, $P_{FWE}=2.027\times10^{-6}$). This was due to decreases in both IA scores ($t(98)=4.226$, $P_{FWE}=2.672\times10^{-5}$) and HI scores ($t(98)=4.394$, $P_{FWE}=1.410\times10^{-5}$), with a mean decrease of 2.04(SD=4.80) in IA, and 1.46(SD=3.30) in HI score.

Symptom change in relation to WM microstructure at two time-points

As a point of reference: Participants who showed relatively more symptom remission had FA values that moved neither towards nor away from that of those who were diagnosed as never affected; their global FA values increased over time at a similar rate as the never affected individuals, while those who essentially persisted or developed more symptoms over time showed a slightly steeper increase in FA than the other two groups (Figure S6).

Our models demonstrated no significant association between combined symptom score remission and FA_{TP1}, but there was a significant negative association between combined symptom score remission and FA_{TP2} in two regions according to the atlas: lSLF($P_{FWE}=0.038$) and lCST($P_{FWE}=0.044$)(Table 2;Figure 3A). This was mainly driven by a negative effect of HI dimension score on FA in lCST($P_{FWE}=0.049$)(Table 2;Figure 3B).

Additionally, there was a negative trend association between combined symptom score difference and FA difference ($P_{FWE}=0.079$). Because our one model with a significant effect, as well as those previously reported in an overlapping sample at an earlier time window, were driven by HI, we performed an exploratory *post-hoc* analysis on symptom score difference and FA difference with only HI dimension scores(Brouwer et al., 2020; Damatac et al., 2020; Francx, Zwiers, et al., 2015). Our exploratory results show that larger HI symptom decrease

237   was associated with a larger decrease in FA over time in ten clusters spread over six WM

238   tracts(Table S2, Figure S7).

239   *Post hoc tests of confounders and demographics*

240   Sex, normalized head motion at respective time point(s), age at TP1, age difference between

241   TP1 and TP2, and CPRS symptom score at TP1 were included as covariates in all models. We

242   report main effects after the removal of non-significant interaction effects in Table 2. We found

243   neither a significant main effect nor an interaction effect of any of these covariates with ΔCPRS

244   for all analyses reported above(Table S3).

Discussion

246   In this longitudinal investigation of ADHD and WM microstructure, we report that higher

247   symptom decrease is associated with lower FA at follow-up in lCST and lSLF, an effect mainly

248   driven by HI symptom decrease. Thereby, we have essentially replicated and extended the

249   findings reported by Francx, Zwiers, et al. (2015) at an older age range, contributing to the

250   growing body of evidence describing the progression of ADHD and its relation with WM.

251   Additionally, we utilized an improved statistical method to account for the family structure in

252   our data, thus confirming that previous results in this cohort were not confounded by within-

253   family correlations(Winkler et al., 2015). By substantiating those earlier findings, with

254   replication in participants at an older age, and upon better accounting for family relatedness,

255   we conclude that a decrease in symptoms from early adolescence is associated with lower FA

256   in late adolescence and young adulthood.

257   Our longitudinal design of two diagnostic and two DWI time-points allows us to

258   speculate about the chronology of brain changes versus symptom changes. First, we found no

259   evidence that baseline FA predicts ADHD symptom change over time. Second, though a

260   natural expectation would be that more remission leads to higher FA, we found the opposite,

261 somewhat paradoxical result: Greater ADHD symptom decrease was associated with lower FA

262 at follow-up in lSLF and lCST. Third, we found that HI, not IA, symptom decrease was the

263 main driver behind the association with reduced FA in lCST. WM microstructure can change

264 in response to behavior or learning (i.e. plasticity). It is possible that decreased (motor)

265 hyperactivity is associated with less use of corticospinal and motor tracts, which may lead to

266 decreased FA in this area at TP2. Overall, lower FA in both tracts appears to follow, rather than

267 precede, symptom decrease. Speculatively, this suggests that the WM changes may be a

268 downstream result, rather than a cause, of symptom remission in ADHD.

269   FA is an indirect reflection of microstructure and some neuronal processes that improve

270 anatomical connectivity may paradoxically manifest as decreased FA in some locations—

271 especially in principal WM highways through which several fibers cross, like the SLF and

272 CST. At the axonal level, more sprouting, pruning, crossing fibers or fiber dispersion in those

273 tracts during maturation may demonstrate as reduced FA over time. Plasticity in myelin or axon

274 integrity in less dominant fibers could also exhibit as reduced FA in voxels containing multiple

275 fiber orientations. In our participants whose symptoms persisted, higher FA could be the

276 outcome of brain reorganization in less dominant fiber tracts, particularly in those that traverse

277 the CST and SLF. Event-related and resting-state functional MRI studies that grouped their

278 subjects categorically have reported that remitters have stronger connectivity than

279 persisters(Clerkin et al., 2013; Francx, Oldehinkel, et al., 2015). Lower functional connectivity

280 in certain tracts may be related to higher FA in other tracts and vice versa. In a top-down

281 fashion, remitters may learn compensatory strategies to overcome their ADHD symptoms as

282 they age, while persisters may either learn disadvantageous strategies, other beneficial

283 compensatory strategies, or none at all, leading to divergent trajectories of WM development

284 in various brain regions in individuals with persistent ADHD symptoms(Wetterling et al.,

285 2015).

286   One can find in the literature several instances wherein the SLF and CST are implicated

287   in ADHD. The SLF generally subserves a wide variety of functions related to language,

288   attention, memory, emotion, and visuospatial function; many studies have pointed to its

289   function in visuospatial awareness, as well as attentional selection of sensory content(Conner

290   et al., 2018; Shaw et al., 2015; Wolfers et al., 2015). Our findings are partly in accordance with

291   those of others that have found neurodevelopmental effects linked with unilaterally

292   compromised lSLF maturation during adolescence(Peters et al., 2012). Thus, ADHD symptom

293   persistence may influence higher unilateral SLF integrity as a person develops from early

294   adolescence to young adulthood. The CST integrates cortical and lower brain processing

295   centers in the motor system, has an important role in modulating sensory information, and may

296   be particularly relevant to motor hyperactivity in ADHD(Moreno-López, Olivares-Moreno,

297   Cordero-Erausquin, & Rojas-Piloni, 2016). Altered modulation of sensory information could

298   potentially be involved in HI remission, as the CST contains fibers running from the primary

299   motor, premotor, supplementary motor, somatosensory, parietal and cingulate cortex to the

300   spine and is thus involved in the control of complex voluntary distal movements(Welniarz,

301   Dusart, & Roze, 2017). Correspondingly, the persistence of HI could, indeed, result in

302   increased FA in CST through time. Our unilateral findings may have risen from the fact that

303   88% of our subjects were right-handed, and most CST axons cross to the contralateral side at

304   the pyramidal decussation before reaching lower motor neurons(Welniarz et al., 2017). We

305   found no evidence that handedness was correlated with change in symptom scores (Table S4).

306   Based on previous investigations that have similarly found effects of ADHD symptoms

307   on WM microstructure driven by HI, we also conducted an exploratory analysis of only HI

308   symptom remission effects on change in FA(Damatac et al., 2020; Francx, Zwiers, et al., 2015).

309   Our results may suggest that HI symptom remission is associated with more decrease in FA

310   over time. Most of the associations we found were clustered in prefrontal and frontostriatal

311   regions. Higher functional connectivity in prefrontal networks in young adults has been

312   associated with more improvement in symptoms over time(Clerkin et al., 2013; Francx, Zwiers,

313   et al., 2015). Likewise, the prefrontal cortex and its connections are especially important in the

314   remission or persistence of ADHD symptoms(Francx, Oldehinkel, et al., 2015; Halperin &

315   Schulz, 2006). As it continues to develop throughout adolescence, the prefrontal cortex can

316   potentially compensate for the initial causes of ADHD through its connectivity with subcortical

317   regions such as the striatum. Indeed, a study using independent component analysis

318   demonstrated that ADHD diagnosis was significantly associated with reduced brain volume in

319   a component that mapped to the frontal lobes, the striatum, and their interconnecting WM

320   tracts(Cupertino et al., 2019). Although exploratory and tentative, our finding of decreased FA

321   in frontostriatal regions coinciding with HI symptom remission is thus in line with Halperin &

322   Schulz's theory (2006): Neural plasticity and the development of the prefrontal cortex and

323   interconnected neural circuits facilitate recovery over the course of development.

324   We used a dimensional approach in defining the ADHD phenotype, in line with our

325   recent findings in a large overlapping cohort wherein no evidence was found for altered FA in

326   association with categorical ADHD diagnosis(Damatac et al., 2020). Unaffected participants

327   clustered at the low end of the score distribution. Given the relatively small number of fully

328   remitted patients (N=5), together with a subset of 'partly remitted' individuals, our use of

329   symptom severity as a continuous variable maximized power to detect symptom-related

330   changes, while also circumventing arbitrary decisions on the definition of remission(Du Rietz

331   et al., 2016). We thus interpret our findings in terms of symptom severity, reflecting the degree

332   of remission in ADHD patients as well as variation in individuals who do not reach diagnostic

333   threshold.

334   Head motion is quite typical in the ADHD population and is hence a common confound

335   in such studies(Aoki et al., 2018; Yendiki, Koldewyn, Kakunoori, Kanwisher, & Fischl, 2014;

336 Zwiers, 2010). A previous meta-analysis of DWI studies in ADHD found that most

337 investigations that controlled for head motion did not have significant results(Aoki et al., 2018).

338 We normalized head motion and included it as a confound covariate in all of our analyses, as

339 well as checked each model for an interaction effect with the head motion parameter. We found

340 no evidence that it had an influence on our results.

341 FA estimates can be less accurate in brain regions consisting of so-called "kissing"

342 and/or crossing fibers, like the CST and SLF. FA gives only one value for the overall restriction

343 of anisotropy in a voxel, which could be a crucial aspect in the inconsistency of findings in the

344 literature regarding WM and ADHD. Future studies may include complementary longitudinal

345 region-of-interest tractography analyses in the clusters that we found to be significant, or by

346 using DWI methods that deliver greater resolution at the neurite level. Techniques that utilize

347 orientation dispersion indices or WM fiber density could potentially provide clarity in the

348 constant discourse of how crossing fibers can mar inferences about FA and brain effects of

349 ADHD. Likewise, incorporating additional DWI data from more than two time points

350 throughout development would, naturally, increase statistical power and enhance our

351 understanding of the dynamic interplay between disorder and development. Due to the wide

352 age range in our sample, we checked for but did not find interactions with baseline age.

353 Nonetheless, more complex, nonlinear patterns with age may exist across the age ranges we

354 studied. We cannot assume that the relationship between symptom change and brain change is

355 a constant process throughout the entire age range in this study.

Conclusion

357 We used two DWI time-points in a longitudinal study of dimensional symptom scores in

358 ADHD. Our results indicate that, in specific WM tracts, greater symptom improvement results

359 in lower FA at follow-up. We show that WM alterations may occur downstream of symptom

360 change. The effects we have found confirm and extend earlier findings in an overlapping

361   sample; they indicate divergent trajectories of WM development in individuals with persistent

362   ADHD symptoms compared to those showing remittance, and support the role of prefrontal

363   and sensorimotor development in the symptom remission of ADHD.

Acknowledgments

Correspondence

371
372   Christienne G. Damatac, Department of Cognitive Neuroscience, Donders Centre for

373   Cognition, Donders Institute for Brain, Cognition and Behaviour, Kapittelweg 29, 6525 EN

374   Nijmegen, The Netherlands; Email: c.gonzalesdamatac@donders.ru.nl

375

Key points

- Attention-deficit hyperactivity disorder is associated with white matter microstructure, but little is known about how they are longitudinally related as a child develops into adulthood.

- We used voxel-wise Tract-Based Spatial Statistics with permutation-based inference to investigate how symptom score change relates to fractional anisotropy in individuals with ADHD and typically developing controls over a period of about four years.

- We provided for the first time, evidence that altered FA appears to follow, rather than precede, changes in symptom remission.

- Our findings indicate divergent white matter developmental trajectories between individuals with persistent and remittent ADHD, and support the role of prefrontal and sensorimotor tracts in the remission of ADHD.

376
377

References

379 American Psychiatric Association. (2013). *American Psychiatric Association, 2013.*

380 *Diagnostic and statistical manual of mental disorders (5th ed.). American Journal of*

381 *Psychiatry*.

382 Aoki, Y., Cortese, S., & Castellanos, F. X. (2018). Research Review: Diffusion tensor

383 imaging studies of attention-deficit/hyperactivity disorder: meta-analyses and reflections

384 on head motion. *Journal of Child Psychology and Psychiatry and Allied Disciplines*,

385 *59*(3), 193–202.

386 Beaulieu, C. (2002). The basis of anisotropic water diffusion in the nervous system - A

387 technical review. *NMR in Biomedicine*, *15*(7–8), 435–455.

388 Brouwer, R. M., Klein, M., Grasby, K. L., Schnack, H. G., Jahanshad, N., Teeuw, J.,

389 Thomopoulos, S. I., et al. (2020). Dynamics of Brain Structure and its Genetic

390 Architecture over the Lifespan. *bioRxiv*.

391   Clerkin, S. M., Schulz, K. P., Berwid, O. G., Fan, J., Newcorn, J. H., Tang, C. Y., &

392   Halperin, J. M. (2013). Thalamo-cortical activation and connectivity during response

393   preparation in adults with persistent and remitted ADHD. *American Journal of*

394   *Psychiatry*, *170*(9), 1011–1019.

395   Conner, A. K., Briggs, R. G., Rahimi, M., Sali, G., Baker, C. M., Burks, J. D., Glenn, C. A.,

396   et al. (2018). A Connectomic Atlas of the Human Cerebrum—Chapter 10: Tractographic

397   Description of the Superior Longitudinal Fasciculus. *Operative Neurosurgery*,

398   *15*(suppl_1), S407–S422.

399   Conners, C. K., Erhardt, D., Epstein, J. N., Parker, J. D. A., Sitarenios, G., & Sparrow, E.

400   (1999). Self-ratings of ADHD symptoms in adults I: Factor structure and normative

401   data. *Journal of Attention Disorders*.

402   Cortese, S., Imperati, D., Zhou, J., Proal, E., Klein, R. G., Mannuzza, S., Ramos-Olazagasti,

403   M. A., et al. (2013). White matter alterations at 33-year follow-up in adults with

404   childhood attention-deficit/hyperactivity disorder. *Biological psychiatry*, *74*(8), 591–8.

405   Retrieved from http://www.ncbi.nlm.nih.gov/pubmed/23566821

406   Cupertino, R. B., Soheili-Nezhad, S., Grevet, E. H., Bandeira, C. E., Picon, F. A., Tavares,

407   M. E., Naaijen, J., et al. (2019). Reduced fronto-striatal volume in ADHD in two cohorts

408   across the lifespan. *bioRxiv*.

409   Damatac, C. G., Chauvin, R. J. M., Zwiers, M. P., van Rooij, D., Akkermans, S. E. A.,

410   Naaijen, J., Hoekstra, P. J., et al. (2020). White Matter Microstructure in Attention-

411   Deficit/Hyperactivity Disorder: A Systematic Tractography Study in 654 Individuals.

412   *Biological Psychiatry: Cognitive Neuroscience and Neuroimaging*, 1–10. Elsevier Inc.

413   Retrieved from https://doi.org/10.1016/j.bpsc.2020.07.015

414   van Duijvenvoorde, A. C. K., Westhoff, B., de Vos, F., Wierenga, L. M., & Crone, E. A.

415   (2019). A three-wave longitudinal study of subcortical–cortical resting-state

416   connectivity in adolescence: Testing age- and puberty-related changes. *Human Brain*

417   *Mapping*, *40*(13), 3769–3783.

418   van Ewijk, H., Heslenfeld, D. J., Zwiers, M. P., Faraone, S. V., Luman, M., Hartman, C. A.,

419   Hoekstra, P. J., et al. (2014). Different mechanisms of white matter abnormalities in

420   attention-deficit/ hyperactivity disorder: A diffusion tensor imaging study. *Journal of the*

421   *American Academy of Child and Adolescent Psychiatry*, *53*(7), 790-799.e3. Elsevier Inc.

422   Retrieved from http://dx.doi.org/10.1016/j.jaac.2014.05.001

423   Faraone, S. V, Asherson, P., Banaschewski, T., Biederman, J., Buitelaar, J. K., Ramos-

424   Quiroga, J. A., Rohde, L. A., et al. (2015). Attention-deficit/hyperactivity disorder.

425   *Nature reviews. Disease primers*, *1*, 15020. Radboud University Medical Center,

426   Donders Institute for Brain, Cognition and Behaviour, Departments of Human Genetics

427   and Psychiatry, Nijmegen, The Netherlands. Retrieved from

428   http://eutils.ncbi.nlm.nih.gov/entrez/eutils/elink.fcgi?dbfrom=pubmed&id=27189265&r

429   etmode=ref&cmd=prlinks

430   Francx, W., Oldehinkel, M., Oosterlaan, J., Heslenfeld, D., Hartman, C. A., Hoekstra, P. J.,

431   Franke, B., et al. (2015). The executive control network and symptomatic improvement

432   in attention-deficit / hyperactivity disorder. *Cortex*, *73*, 62–72. Elsevier Srl. Retrieved

433   from http://dx.doi.org/10.1016/j.cortex.2015.08.012

434   Francx, W., Zwiers, M. P., Mennes, M., Oosterlaan, J., Heslenfeld, D., Hoekstra, P. J.,

435   Hartman, C. A., et al. (2015). White matter microstructure and developmental

436   improvement of hyperactive/impulsive symptoms in attention-deficit/hyperactivity

437   disorder. *Journal of Child Psychology and Psychiatry and Allied Disciplines*, *56*(12),

438   1289–1297. Karakter Child and Adolescent Psychiatry University Centre, Nijmegen,

439   The Netherlands. Retrieved from http://doi.wiley.com/10.1111/jcpp.12379

440   Franke, B., Michelini, G., Asherson, P., Banaschewski, T., Bilbow, A., Buitelaar, J. K.,

441   Cormand, B., et al. (2018). Live fast , die young ? A review on the developmental

442   trajectories of ADHD across the lifespan. *European Neuropsychopharmacology*, *28*(10),

443   1059–1088. Elsevier B.V. Retrieved from

444   https://doi.org/10.1016/j.euroneuro.2018.08.001

445   Giorgio, A., Watkins, K. E., Douaud, G., James, A. C., James, S., De Stefano, N., Matthews,

446   P. M., et al. (2008). Changes in white matter microstructure during adolescence.

447   *NeuroImage*, *39*(1), 52–61.

448   Halperin, J. M., & Schulz, K. P. (2006). Revisiting the role of the prefrontal cortex in the

449   pathophysiology of attention-deficit/hyperactivity disorder. *Psychological bulletin*,

450   *132*(4), 560–581. Department of Psychology, Queens College of the City University of

451   New York, Flushing, NY 11367, USA. jeffrey.halperin@qc.cuny.edu. Retrieved from

452   http://eutils.ncbi.nlm.nih.gov/entrez/eutils/elink.fcgi?dbfrom=pubmed&id=16822167&r

453   etmode=ref&cmd=prlinks

454   Hoogman, M., Bralten, J., Hibar, D. P., Mennes, M., Zwiers, M. P., Schweren, L. S. J., van

455   Hulzen, K. J. E., et al. (2017). Subcortical brain volume differences in participants with

456   attention deficit hyperactivity disorder in children and adults: a cross-sectional mega-

457   analysis. *The Lancet Psychiatry*, *4*(4), 310–319.

458   Kochunov, P., Williamson, D. E., Lancaster, J., Fox, P., Cornell, J., Blangero, J., & Glahn, D.

459   C. (2012). Fractional anisotropy of water diffusion in cerebral white matter across the

460   lifespan. *Neurobiology of Aging*, *33*(1), 9–20. Retrieved from

461   https://linkinghub.elsevier.com/retrieve/pii/S0197458010000448

462   Lahey, B. B., & Willcutt, E. G. (2010). Predictive Validity of a Continuous Alternative to

463   Nominal Subtypes of Attention-Deficit/Hyperactivity Disorder for DSM – V. *Journal of*

464   *Clinical Child & Adolescent Psychology*, *39*(6), 761–775. Retrieved from

465   http://www.tandfonline.com/doi/abs/10.1080/15374416.2010.517173

466 Lebel, C., & Deoni, S. (2018). The development of brain white matter microstructure.

467 *NeuroImage*, *182*(3), 207–218. Retrieved from

468 https://linkinghub.elsevier.com/retrieve/pii/S1053811917311217

469 Madhyastha, T., Mérillat, S., Hirsiger, S., Bezzola, L., Liem, F., Grabowski, T., & Jäncke, L.

470 (2014). Longitudinal reliability of tract-based spatial statistics in diffusion tensor

471 imaging. *Human Brain Mapping*, *35*(9), 4544–4555.

472 Marcus, D. K., & Barry, T. D. (2011). Does attention-deficit/hyperactivity disorder have a

473 dimensional latent structure? A taxometric analysis. *Journal of Abnormal Psychology*,

474 *120*(2), 427–442. Retrieved from http://doi.apa.org/getdoi.cfm?doi=10.1037/a0021405

475 Moreno-López, Y., Olivares-Moreno, R., Cordero-Erausquin, M., & Rojas-Piloni, G. (2016).

476 Sensorimotor integration by corticospinal system. *Frontiers in Neuroanatomy*,

477 *10*(MAR), 1–6.

478 Müller, U. C., Asherson, P., Banaschewski, T., Buitelaar, J. K., Ebstein, R. P., Eisenberg, J.,

479 Gill, M., et al. (2011a). The impact of study design and diagnostic approach in a large

480 multi-centre ADHD study. Part 1: ADHD symptom patterns. *BMC Psychiatry*, *11*(1),

481 54. BioMed Central Ltd. Retrieved from

482 http://bmcpsychiatry.biomedcentral.com/articles/10.1186/1471-244X-11-54

483 Müller, U. C., Asherson, P., Banaschewski, T., Buitelaar, J. K., Ebstein, R. P., Eisenberg, J.,

484 Gill, M., et al. (2011b). The impact of study design and diagnostic approach in a large

485 multi-centre ADHD study: Part 2: Dimensional measures of psychopathology and

486 intelligence. *BMC Psychiatry*, *11*(1), 55. BioMed Central Ltd.

487 Paus, T., Collins, D. L., Evans, A. C., Leonard, G., Pike, B., & Zijdenbos, A. (2001).

488 Maturation of white matter in the human brain: A review of magnetic resonance studies.

489 *Brain Research Bulletin*, *54*(3), 255–266.

490 Peters, B. D., Szeszko, P. R., Radua, J., Ikuta, T., Gruner, P., Derosse, P., Zhang, J. P., et al.

491   (2012). White matter development in adolescence: Diffusion tensor imaging and meta-

492   analytic results. *Schizophrenia Bulletin*, *38*(6), 1308–1317.

493 von Rhein, D., Mennes, M., van Ewijk, H., Groenman, A. P., Zwiers, M. P., Oosterlaan, J.,

494   Heslenfeld, D., et al. (2015). The NeuroIMAGE study: a prospective phenotypic,

495   cognitive, genetic and MRI study in children with attention-deficit/hyperactivity

496   disorder. Design and descriptives. *European Child and Adolescent Psychiatry*, *24*(3),

497   265–281. Centre for Cognitive Neuroscience, Donders Institute for Brain, Cognition and

498   Behaviour, Radboud University Medical Centre, Nijmegen, The Netherlands,

499   Daniel.vonRhein@gmail.com. Retrieved from

500   http://eutils.ncbi.nlm.nih.gov/entrez/eutils/elink.fcgi?dbfrom=pubmed&id=25012461&r

501   etmode=ref&cmd=prlinks

502 Du Rietz, E., Cheung, C. H. M., McLoughlin, G., Brandeis, D., Banaschewski, T., Asherson,

503   P., & Kuntsi, J. (2016). Self-report of ADHD shows limited agreement with objective

504   markers of persistence and remittance. *Journal of Psychiatric Research*.

505 Shaw, P., Sudre, G., Wharton, A., Weingart, D., Sharp, W., & Sarlls, J. (2015). White matter

506   microstructure and the variable adult outcome of childhood attention deficit

507   hyperactivity disorder. *Neuropsychopharmacology*, *40*(3), 746–754. Nature Publishing

508   Group. Retrieved from http://dx.doi.org/10.1038/npp.2014.241

509 Smith, S. M., Jenkinson, M., Johansen-berg, H., Rueckert, D., Nichols, T. E., Mackay, C. E.,

510   Watkins, K. E., et al. (2006). Tract-based spatial statistics: Voxelwise analysis of multi-

511   subject diffusion data. *NeuroImage*, *31*(4), 1487–1505.

512 Smith, S. M., & Nichols, T. E. (2009). Threshold-free cluster enhancement: Addressing

513   problems of smoothing, threshold dependence and localisation in cluster inference.

514   *NeuroImage*, *44*(1), 83–98. Elsevier Inc.

515 Sudre, G., Mangalmurti, A., & Shaw, P. (2018). Growing out of attention deficit

516   hyperactivity disorder: Insights from the 'remitted' brain. *Neuroscience and*

517   *Biobehavioral Reviews*, *94*(September), 198–209.

518 Welniarz, Q., Dusart, I., & Roze, E. (2017). The corticospinal tract: Evolution, development,

519   and human disorders. *Developmental Neurobiology, 77*(7), 810–829.

520 Wetterling, F., Mccarthy, H., Tozzi, L., Skokauskas, N., O'Doherty, J. P., Mulligan, A.,

521   Meaney, J., et al. (2015). Impaired reward processing in the human prefrontal cortex

522   distinguishes between persistent and remittent attention deficit hyperactivity disorder.

523   *Human Brain Mapping*, *36*(11), 4648–4663.

524 Winkler, A. M., Ridgway, G. R., Webster, M. A., Smith, S. M., & Nichols, T. E. (2014).

525   Permutation inference for the general linear model. *NeuroImage*, *92*, 381–397. The

526   Authors.

527 Winkler, A. M., Webster, M. A., Vidaurre, D., Nichols, T. E., & Smith, S. M. (2015). Multi-

528   level block permutation. *NeuroImage*, *123*, 253–268. The Authors.

529 Wolfers, T., Onnink, A. M. H., Zwiers, M. P., Arias-Vasquez, A., Hoogman, M., Mostert, J.

530   C., Kan, C. C., et al. (2015). Lower white matter microstructure in the superior

531   longitudinal fasciculus is associated with increased response time variability in adults

532   with attentiondeficit/hyperactivity disorder. *Journal of Psychiatry and Neuroscience*,

533   *40*(5), 344–351.

534 Yendiki, A., Koldewyn, K., Kakunoori, S., Kanwisher, N., & Fischl, B. (2014). Spurious

535   group differences due to head motion in a diffusion MRI study. *NeuroImage*, *88*(88),

536   79–90. Retrieved from https://linkinghub.elsevier.com/retrieve/pii/S1053811913011312

537 Zwiers, M. P. (2010). NeuroImage Patching cardiac and head motion artefacts in diffusion-

538   weighted images. *NeuroImage*, *53*(2), 565–575. Elsevier Inc. Retrieved from

539   http://dx.doi.org/10.1016/j.neuroimage.2010.06.014

540

541 **Figures and tables**

542

|	TP1		TP2			
	Mean	**(SD)**	**Mean**	**(SD)**	**Test Statistic**	**(P)**
Age, years	16.91	(3.47)	20.57	(3.52)		
Sex, female	N = 42	42%	N = 42	42%		
Estimated IQ	105.15	(15.02)	106.44	(16.38)	$F(1,100) = 0.84$	(0.38)
Head motion, framewise displacement	0.51	(0.35)	0.47	(0.22)	$F(1,100) = 2.41$	($<10^{-4}$)
Handedness, right	N = 89	89%	N = 89	89%		
CPRS dimension score by diagnostic group						
Combined score	12.76	(12.11)	9.26	(10.20)		
Affected	24.38	(9.63)	18.86	(10.03)		
Subthreshold	8.55	(7.79)	7.13	(7.55)		
Unaffected	4.04	(4.40)	3.06	(4.07)		
Inattention score	8.05	(7.65)	6.02	(6.65)		
Affected	15.05	(5.98)	12.17	(6.55)		
Subthreshold	5.64	(5.35)	4.53	(4.44)		
Unaffected	2.76	(3.82)	2.06	(3.14)		
Hyperactivity-impulsivity score	4.71	(5.30)	3.25	(4.23)		
Affected	9.32	(5.28)	6.69	(4.88)		
Subthreshold	2.91	(3.05)	2.60	(3.20)		
Unaffected	1.28	(1.64)	1.00	(1.65)		
Medication use						
Duration, cumulative days	668	(1,056)	1,161	(1,720)		
Ever used, yes	N = 46	46%	N = 46	46%		

543

544   **Table 1.** Demographic and clinical characteristics of the sample at NeuroIMAGE1(TP1) and

545   NeuroIMAGE2(TP2) with mean and standard deviation. Reported values pertain to all participants in the final

546   sample after all quality control(N=99). IQ: estimated at both timepoints using vocabulary and block design

547   subtests of the Wechsler Intelligence Scale for Children(WISC-III) or Wechsler Adult Intelligence Scale(WAIS-

548   III). Combined CPRS symptom score is the sum of two separate dimensions: hyperactivity-impulsivity and

549   inattention. Medications: Ritalin(methylphenidate), Concerta(methylphenidate), Strattera(atomoxetine), and any

550   other ADHD medication. The majority of patients were taking prescription medication for ADHD, mostly

551   methylphenidate or atomoxetine. Medication use duration: lifetime cumulative number of days used on the day

552   of the MRI scan (numerical integer value). Ever used: whether or not participants had ever taken ADHD

553   medication in their lives (binary factor: yes or no).

554

555

| Model	WM tract	N_{voxels}	MNI (Peak voxel)			t_{max}	P_{FWE}
			X_{COG}	Y_{COG}	Z_{COG}		
$FA_{TP2} \sim \Delta CPRS_{combined}$	lCST	723	-21	-27	44	0.755	**0.044**
	lSLF	579	-33	-20	38	0.881	**0.038**
$FA_{TP2} \sim \Delta CPRS_{HI}$	lCST	17	-18	-25	52	0.981	**0.049**

556

557 **Table 2.** TBSS results of significant models: WM tracts, peak voxels, and localization of significant

558 clusters(P_{FWE}<0.05) of voxel-wise permutation based dimensional analyses (see full composition of models in

559 Table S1). N_{voxels}: number of voxels, X/Y/Z_{COG}: location of the center of gravity for the cluster(vox/mm), MNI:

560 Montreal Neurological Institute coordinates, t_{max}: highest threshold-free cluster enhancement t-statistic value per

561 cluster, WM tract: anatomical location in a white matter tract based on the Johns Hopkins University DTI-based

562 white-matter atlases, lCST: left corticospinal tract, lSLF: left superior longitudinal fasciculus. Model $FA_{TP2} \sim$

563 $\Delta CPRS_{combined}$: Less combined symptom score decrease was associated with more FA at follow-up in lSLF and

564 lCST. Model $FA_{TP2} \sim \Delta CPRS_{HI}$: The negative effect in the previous model was driven by HI score remission.
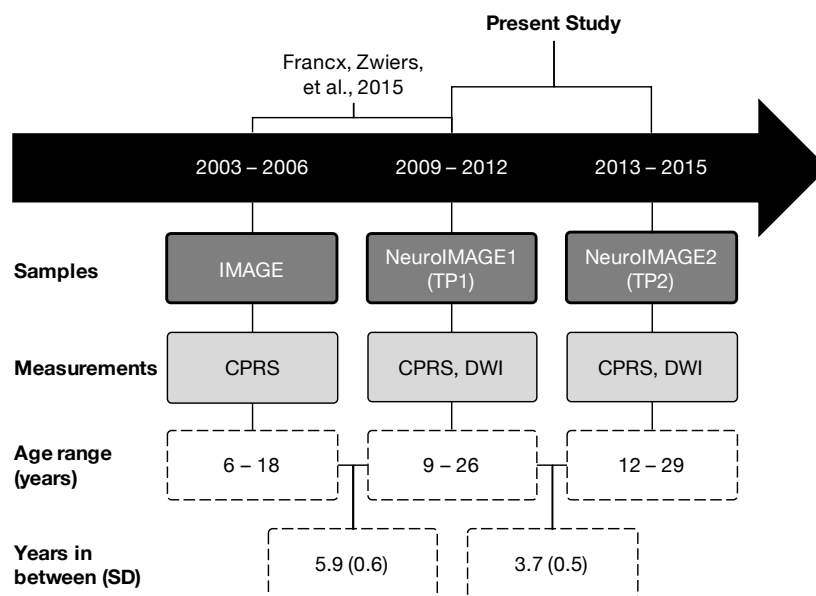
Figure 1. Schematic diagram of how this study chronologically relates to a previous study, samples included, relevant clinical and imaging measurements, study sample age ranges, and mean years (standard deviation) in between each measurement time-point(Francx, Zwiers, et al., 2015; Müller et al., 2011b; von Rhein et al., 2015). The present study is an analysis of TP1 and TP2. DWI: diffusion-weighted imaging, CPRS: Conners Parent Rating Scale(Conners et al., 1999).
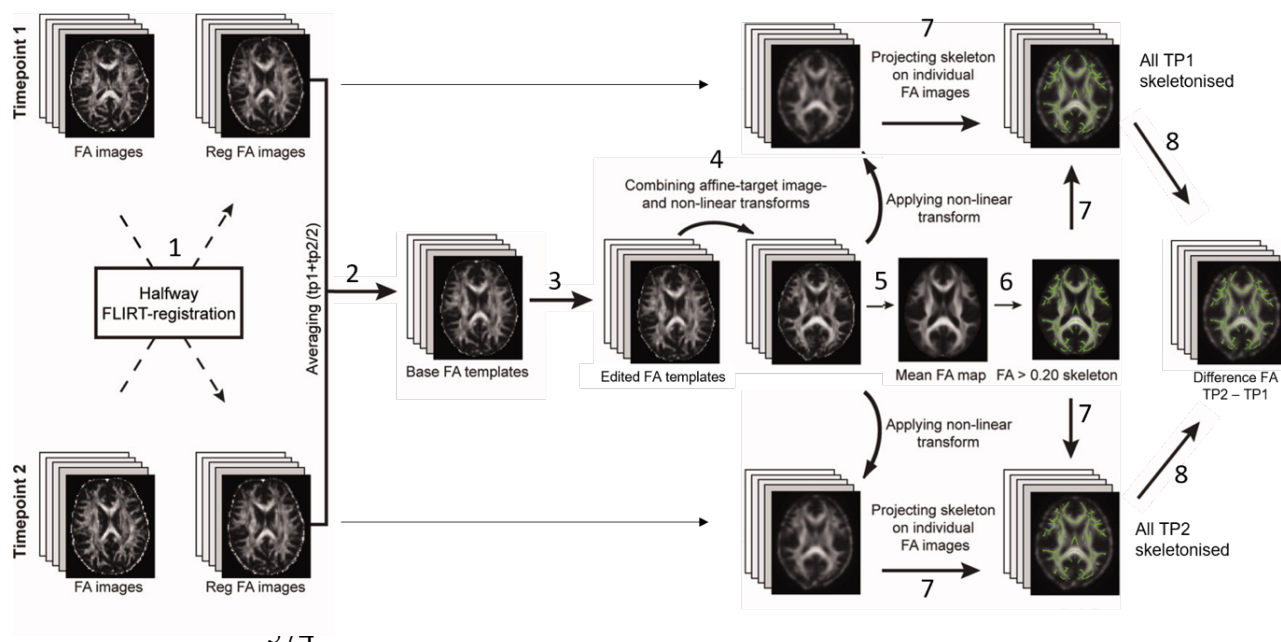
Figure 2. Our longitudinal TBSS pipeline was adapted to create a nonbiased individual subject template for use as a base template (2), which was then non-linearly registered to FMRIB58 FA standard-space (4), to create a mean FA skeleton (5), onto which each subject's aligned FA data from both time points was projected (7).

579

580
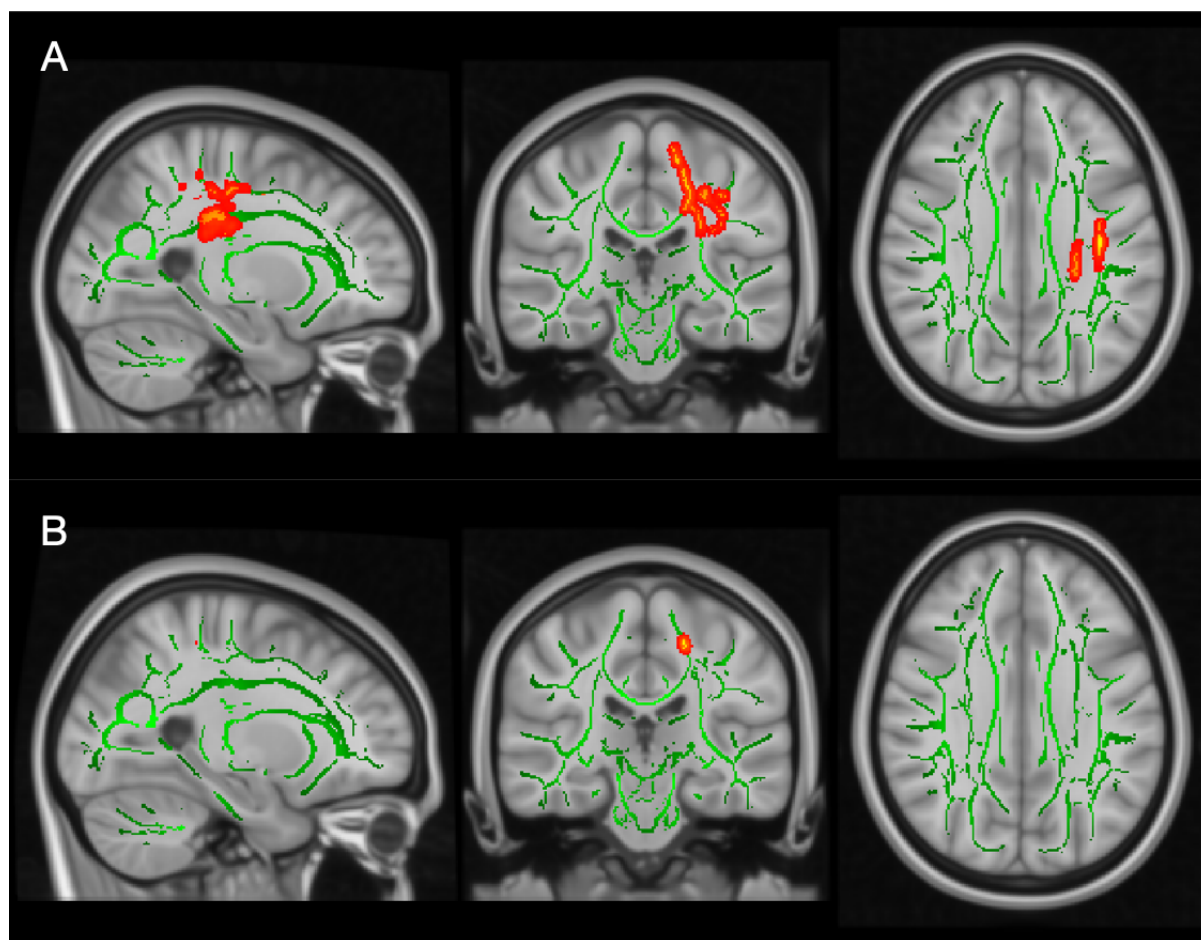
Figure 3. TBSS results showing significant associations (red-yellow) between FA values and the CPRS

dimension scores over time. The mean FA skeleton across all subjects (green) was overlain on the MNI template

image for presentation (x=-25, y=-25, z=31). Results were thickened for visualization (FSL "tbss_fill") and

presented here in radiological convention from sagittal, coronal, and axial perspectives, respectively. **(A)** Lower

FA values at follow-up (TP2) were associated with a larger decrease in combined symptom score in the left

superior longitudinal fasciculus (lSLF)(P_{FWE}=0.038) and the left corticospinal tract (lCST)(P_{FWE}=0.044);

(B) Lower FA values at TP2 were associated with a larger decrease in HI symptom score in lCST(P_{FWE}=0.049).

588

589 ## Supplementary materials

590

Model 1	$FA_{TP1} \sim \Delta CPRS + age_{TP1} + \Delta age + sex + CPRS_{TP1} + head\ motion_{TP1}$
Model 2	$FA_{TP2} \sim \Delta CPRS + age_{TP1} + \Delta age + sex + CPRS_{TP1} + head\ motion_{TP2}$
Model 3	$\Delta FA \sim \Delta CPRS + age_{TP1} + \Delta age + sex + CPRS_{TP1} + head\ motion_{TP1} + head\ motion_{TP2}$

591

592 **Table S1.** Composition of our three general linear models. We essentially have a cross-lagged design with

593 fractional anisotropy (FA) as the dependent variable. The difference in CPRS ($\Delta CPRS = CPRS_{TP1} - CPRS_{TP2}$) is

594 the predictor variable in all models. For each model, CPRS score could be the inattention, hyperactivity-

595 impulsivity, or combined score. The outcome variables of these models are, respectively: FA at baseline (TP1),

596 FA at follow-up (TP2), and change in FA. Permutation analysis (PALM) necessitated that we kept the (TBSS

597 output) FA image as the dependent variable. We covaried for participant baseline age, change in years of age,

598 sex, baseline CPRS symptom score, and framewise displacement head motion at the relevant FA time-point in

599 the dependent variable.

600

601

Exploratory model	WM tract	N_{voxels}	MNI (Peak voxel)			t_{max}	P_{FWE}
			X_{COG}	Y_{COG}	Z_{COG}		
$\Delta FA \sim \Delta CPRS_{HI}$	lIFOF	508	-29	24	17	0.441	0.041
	lIFOF	376	-17	31	-10	0.613	0.035
	Fmin	339	-18	50	0	0.585	0.042
	lUNC	174	-25	17	-8	0.564	0.045
	lCST	158	-22	-13	8	0.562	0.047
	Fmin	22	-20	38	21	0.563	0.049
	CCG	17	-17	32	23	0.562	0.049
	lIFOF	11	-28	15	-1	0.563	0.049
	Fmin	11	-18	46	17	0.566	0.049
	Fmin	9	-12	41	-17	0.563	0.049

602

603 **Table S2.** Exploratory *post-hoc* analysis results. Greater HI symptom decrease was associated with a larger

604 decrease in FA over time in several WM clusters. P-values reported here were not adjusted for multiple testing.

605 lIFOF: left inferior fronto-occipital fasciculus, Fmin: forceps minor of the corpus callosum, lUNC: left uncinate

606 fasciculus, CCG: cingulum cingulate gyrus.

607

608

Model	WM tract	MNI (Peak voxel)						age$_{TP1}$ interaction P
		N_{voxels}	X_{COG}	Y_{COG}	Z_{COG}	t_{max}	P_{FWE}	
FA$_{TP2}$ ~ ΔCPRS$_{combined}$	lCST	723	-21	-27	44	0.755	0.044	0.463
	lSLF	579	-33	-20	38	0.881	0.038	0.808
FA$_{TP2}$ ~ ΔCPRS$_{HI}$	lCST	17	-18	-25	52	0.981	0.049	0.154
ΔFA ~ ΔCPRS$_{HI}$	lIFOF	508	-29	24	17	0.441	0.041	0.667
	lIFOF	376	-17	31	-10	0.613	0.035	0.055
	Fmin	339	-18	50	0	0.585	0.042	0.874
	lUNC	174	-25	17	-8	0.564	0.045	0.131
	lCST	158	-22	-13	8	0.562	0.047	0.130
	Fmin	22	-20	38	21	0.563	0.049	0.239
	CCG	17	-17	32	23	0.562	0.049	0.238
	lIFOF	11	-28	15	-1	0.563	0.049	0.238
	Fmin	11	-18	46	17	0.566	0.049	0.239
	Fmin	9	-12	41	-17	0.563	0.049	0.237

609

610 **Table S3.** Interaction effects of ΔCPRS and age at TP1 for significant models.

611

612

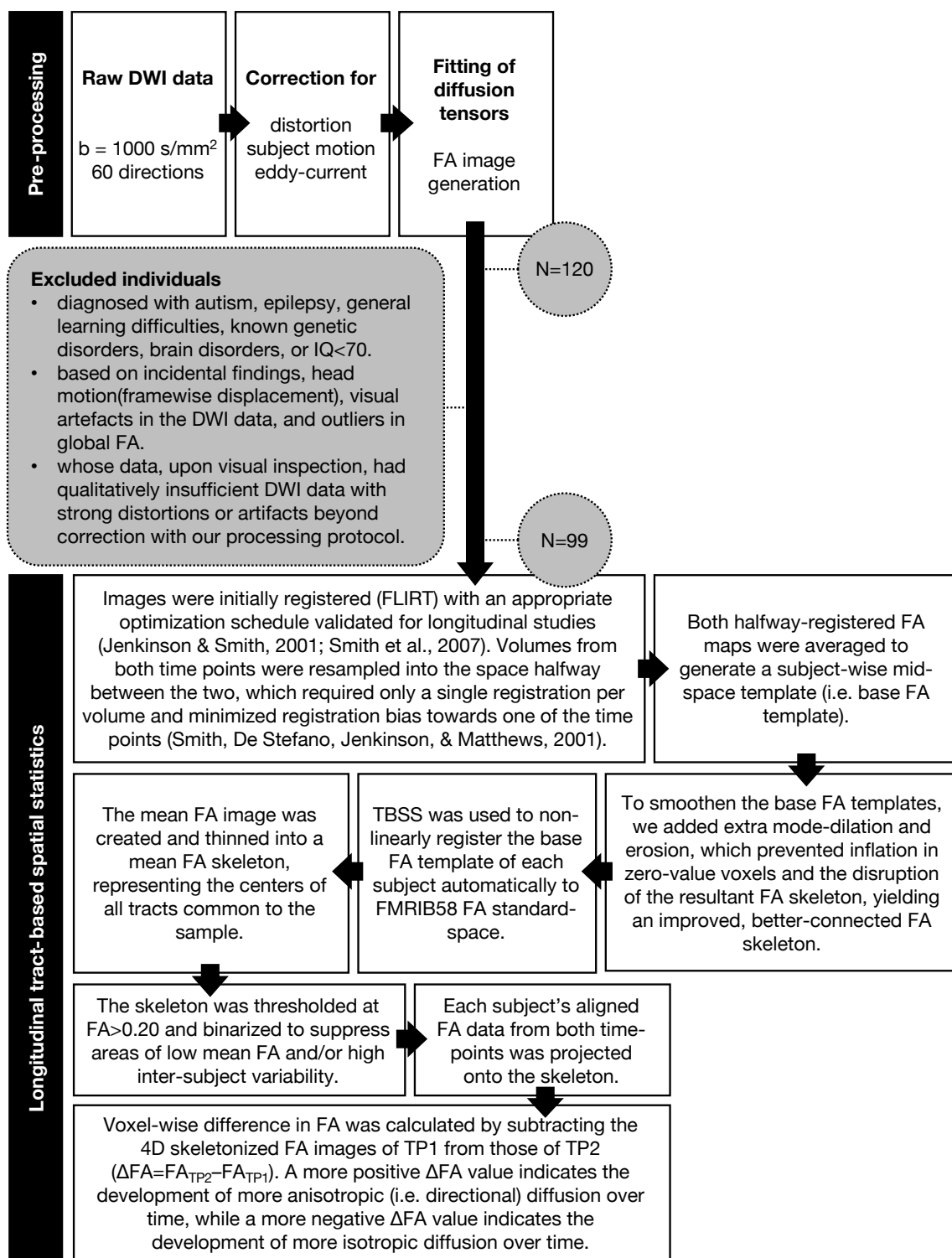| ΔCPRS score	Spearman's ρ	*P*
Combined	0.038	0.709
Hyperactivity-impulsivity	0.098	0.331
Inattention	-0.007	0.948

613

614 **Table S4.** No significant correlation (Spearman's rho) between difference in CPRS score (ΔCPRS=CPRS$_{TP1}$–

615 CPRS$_{TP2}$) and right-handedness in our sample.

616

Pre-processing

Raw DWI data	Correction for	Fitting of diffusion tensors
b = 1000 s/mm^2 60 directions	distortion subject motion eddy-current	FA image generation

Excluded individuals
- diagnosed with autism, epilepsy, general learning difficulties, known genetic disorders, brain disorders, or IQ<70.
- based on incidental findings, head motion(framewise displacement), visual artefacts in the DWI data, and outliers in global FA.
- whose data, upon visual inspection, had qualitatively insufficient DWI data with strong distortions or artifacts beyond correction with our processing protocol.

N=120

N=99

Longitudinal tract-based spatial statistics

Images were initially registered (FLIRT) with an appropriate optimization schedule validated for longitudinal studies (Jenkinson & Smith, 2001; Smith et al., 2007). Volumes from both time points were resampled into the space halfway between the two, which required only a single registration per volume and minimized registration bias towards one of the time points (Smith, De Stefano, Jenkinson, & Matthews, 2001).

Both halfway-registered FA maps were averaged to generate a subject-wise mid-space template (i.e. base FA template).

To smoothen the base FA templates, we added extra mode-dilation and erosion, which prevented inflation in zero-value voxels and the disruption of the resultant FA skeleton, yielding an improved, better-connected FA skeleton.

The mean FA image was created and thinned into a mean FA skeleton, representing the centers of all tracts common to the sample.

TBSS was used to non-linearly register the base FA template of each subject automatically to FMRIB58 FA standard-space.

The skeleton was thresholded at FA>0.20 and binarized to suppress areas of low mean FA and/or high inter-subject variability.

Each subject's aligned FA data from both time-points was projected onto the skeleton.

Voxel-wise difference in FA was calculated by subtracting the 4D skeletonized FA images of TP1 from those of TP2 ($\Delta FA = FA_{TP2} - FA_{TP1}$). A more positive ΔFA value indicates the development of more anisotropic (i.e. directional) diffusion over time, while a more negative ΔFA value indicates the development of more isotropic diffusion over time.

617
618 **Figure S1.** Processing pipeline. During pre-processing, DWI images were realigned and corrected for residual

619 eddy current and for motion artefacts using robust tensor modelling (PATCH)(Zwiers, 2010). Diffusion tensor

620 characteristics and FA values were calculated for each voxel(Behrens et al., 2003). After pre-processing, we

621 used a custom longitudinal TBSS pipeline adapted from others to create non-biased individual subject templates
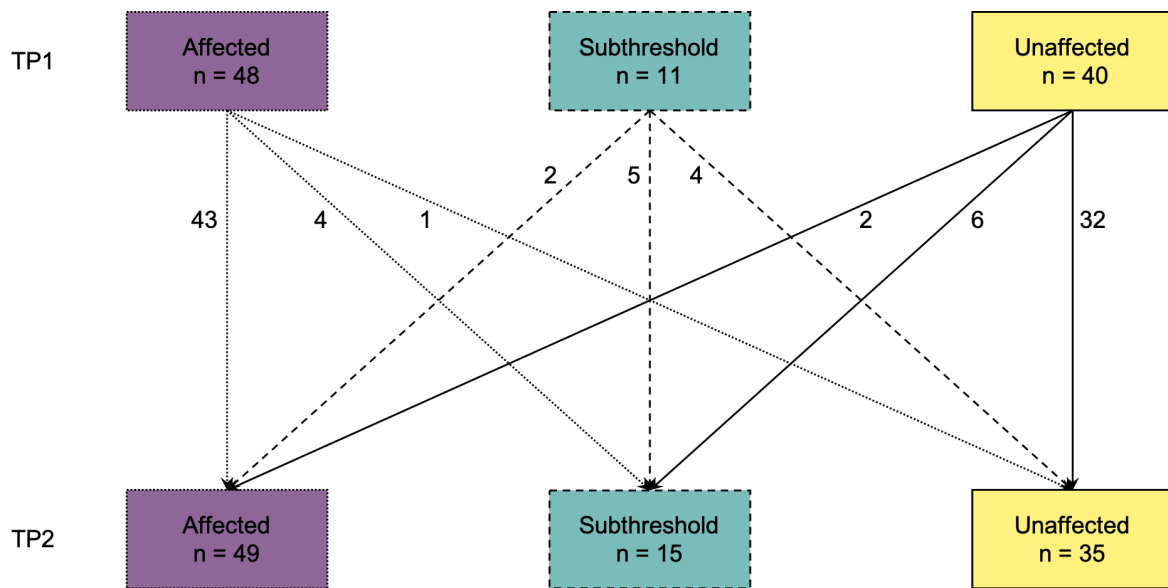
622 (Madhyastha et al., 2014).

623
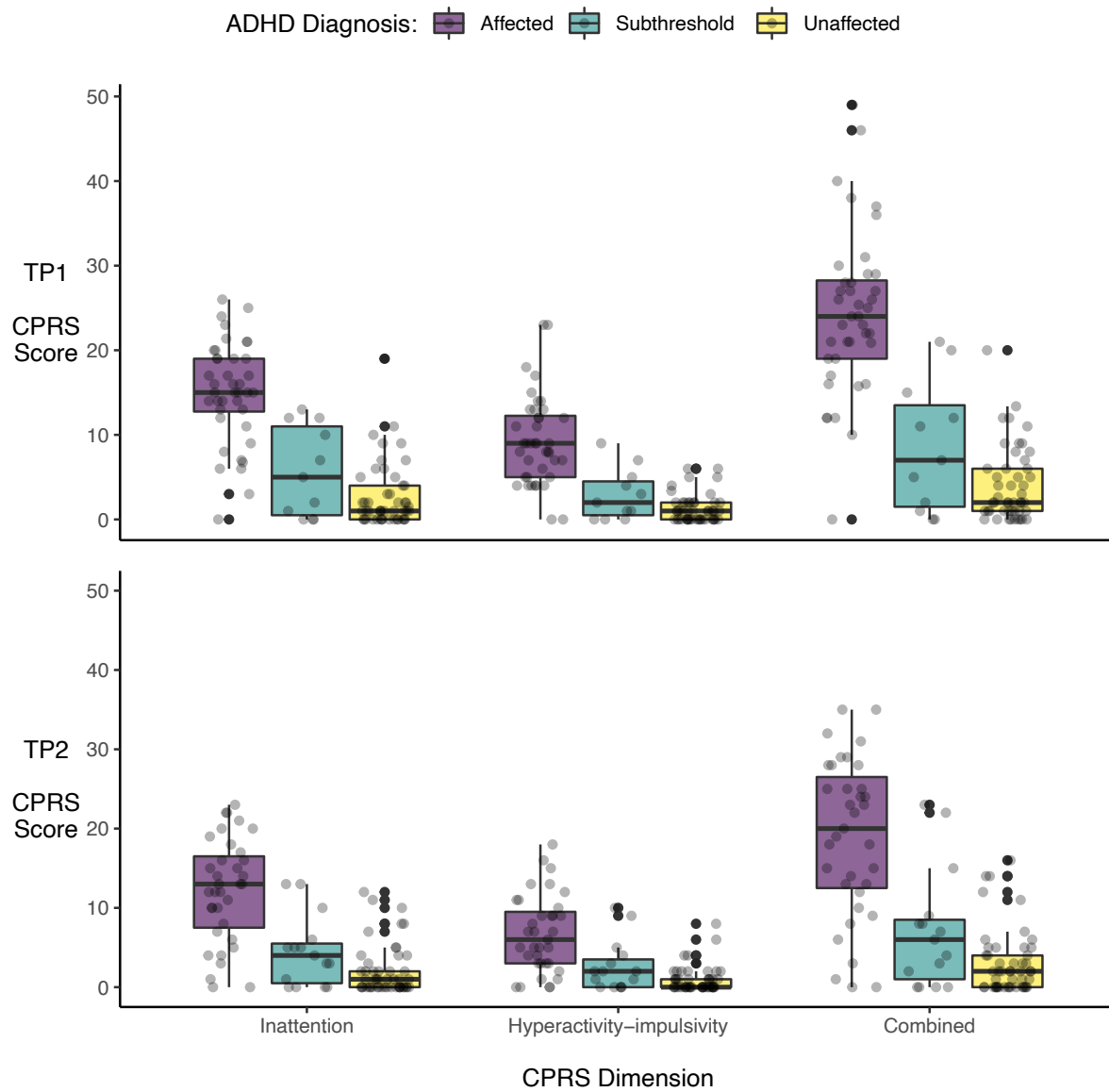
Figure S2. Jittered scatterplots overlain with boxplots of individual Conners Parent Rating Scale (CPRS) dimension scores colored by clinical diagnosis group at baseline (TP1; top panel) and follow-up (TP2; bottom panel).
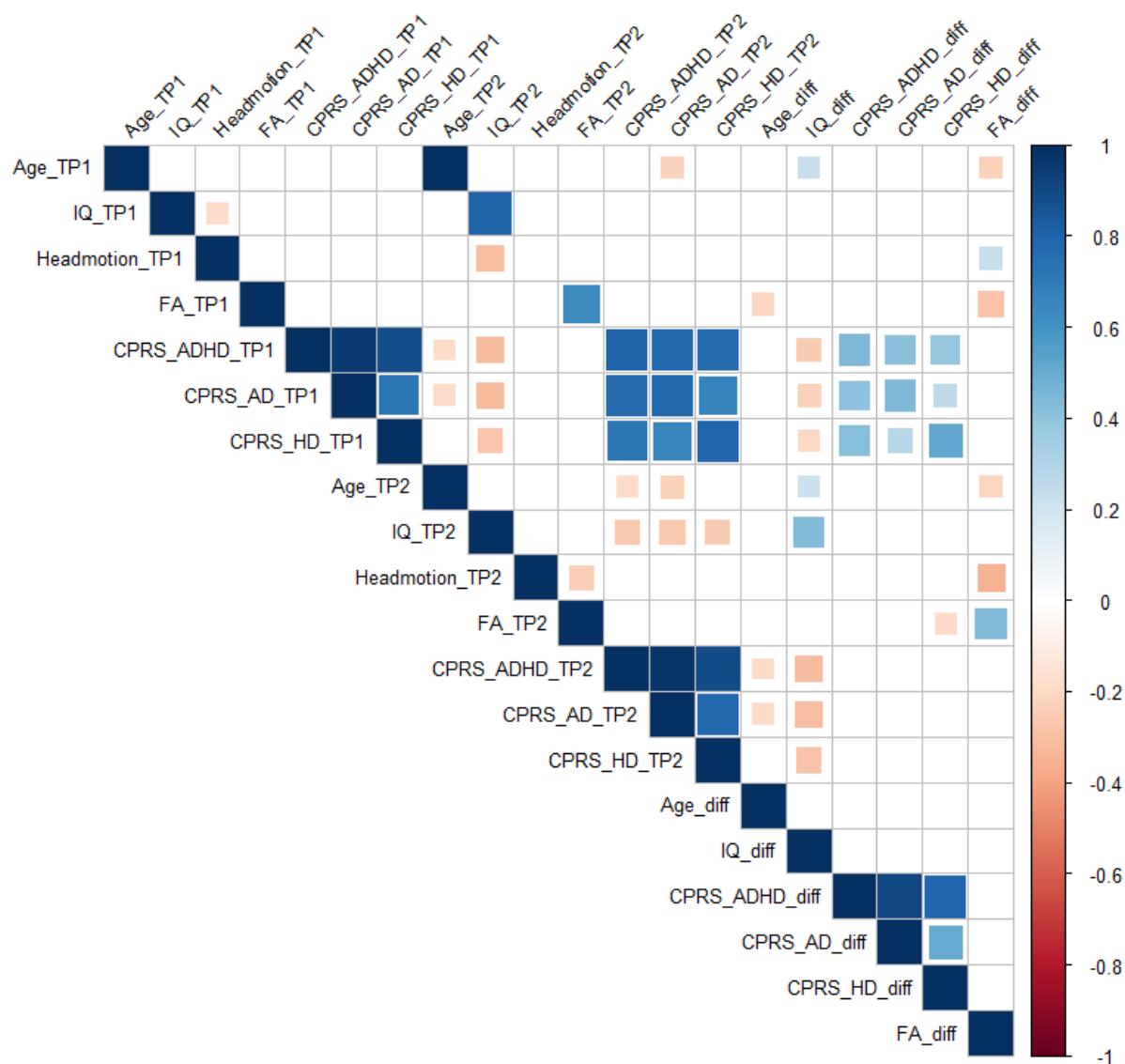
Figure S3. Changes in the diagnostic make-up of our study sample (N=99). Although the total number of participants remained constant, the number of individuals in each diagnosis group changed between time-point 1 (TP1) and time-point 2 (TP2).

636
637   **Figure S4.** Spearman correlation matrix of independent and dependent variables, as well as covariates. These

638   correlation tests were performed before the main analyses. The color intensity of each box indicates the

639   magnitude of the correlation. Positive correlations are presented in blue and negative correlations in red. The

640   size of the box indicates its significance, with significant correlations filling each square completely.

641
642
643
644
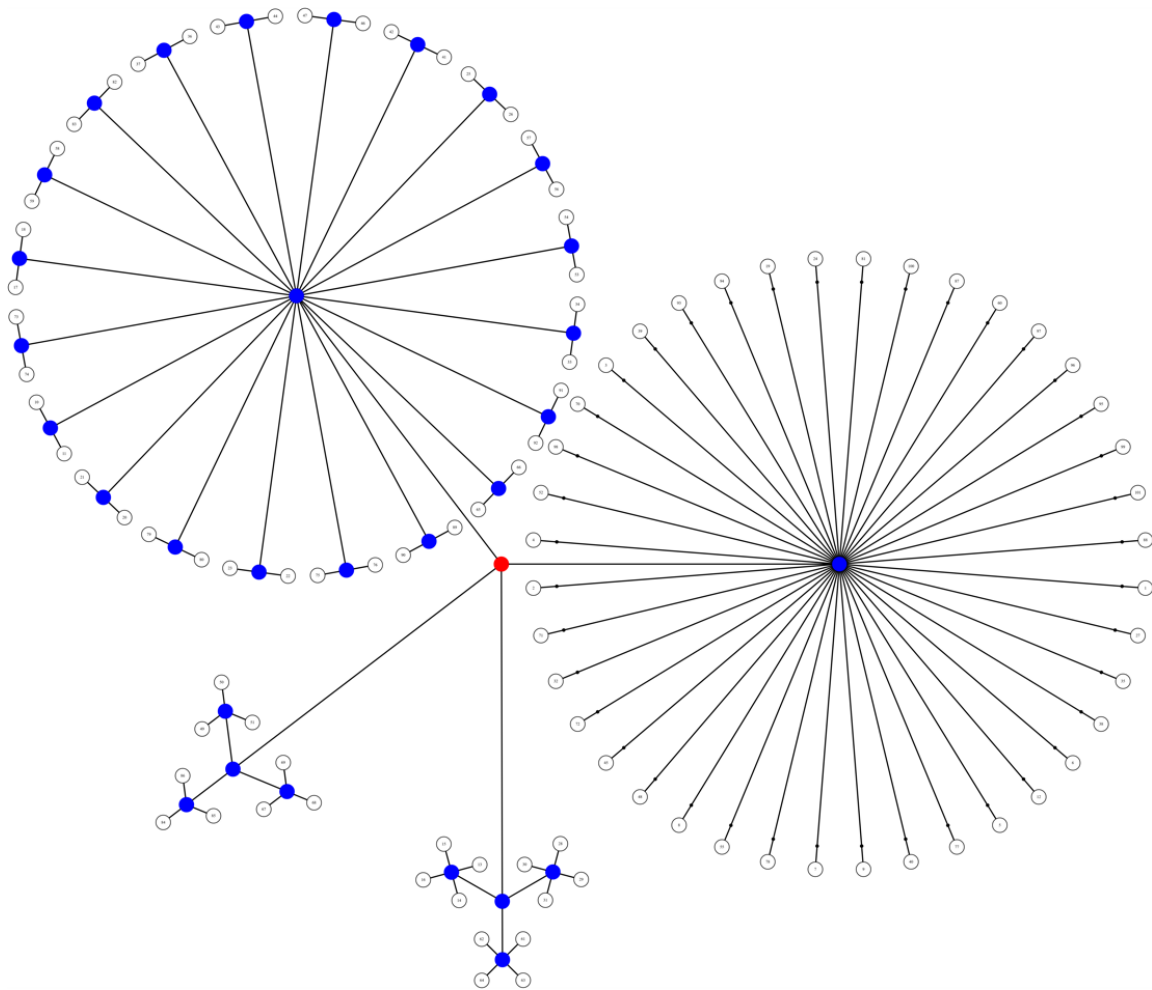
645
646
647   **Figure S5.** Visual representation of the multi-level notation of family structure in our sample. The four groups

648   represent the size of each family: 3 families of 3 children, 3 families of 4 children, 20 families of 2 children, and

649   40 families of 1 child in the study. We depict the levels as branches from the central red node, akin to a tree in

650   which the most peripheral elements (leaves) represent the observations. The nodes from which the branches

651   depart either allow (blue) or do not allow (red) permutations.

652

653
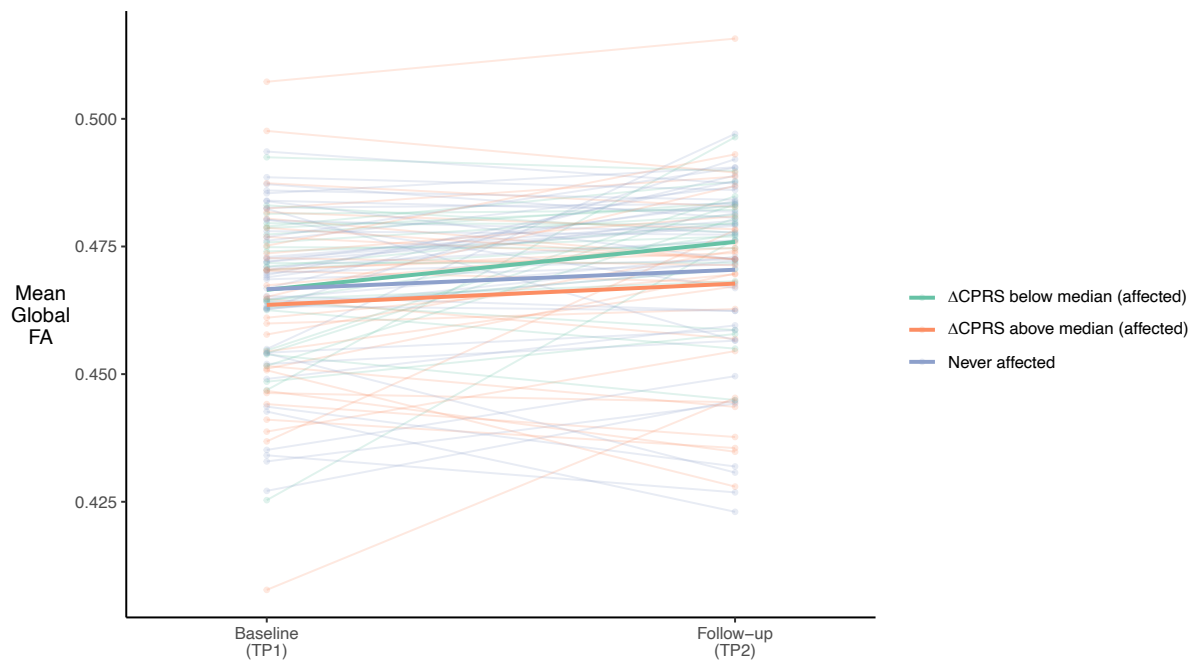
654
655
656 **Figure S6.** Line plot illustrating individual changes in average whole-brain fractional anisotropy (FA) from

657 baseline to follow-up, grouped by never affected participants (blue) versus affected participants (including

658 subthreshold). Here, affected individuals are further split along the median into two groups according to whether

659 their change in combined Conners Parent Rating Scale score (ΔCPRS) was above (orange) or below (green) the

660 affected sample's median of that change.

661

662
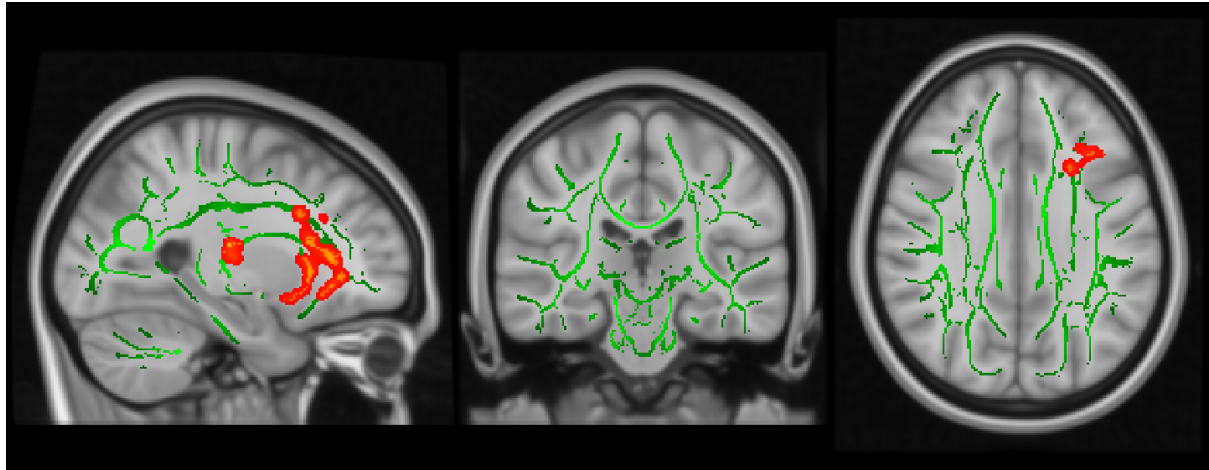
Figure S7. Exploratory dimensional TBSS analyses showing significant associations (red-yellow) between FA

values and the CPRS scores over time. The mean FA skeleton across all subjects (green) was overlain on the

MNI template image for presentation (x=-25, y=-25, z=31). Results were thickened for visualization (FSL

"tbss_fill") and presented here in radiological convention from sagittal, coronal, and axial perspectives,

respectively. A more negative change in FA (i.e. more isotropic diffusion) over time was associated with more

HI symptom remission in ten clusters spread over six WM tracts. See Table S2 for cluster statistics and

locations.